AAPS PharmSciTech, Vol. 16, No. 1, February 2015 (© 2014)
DOI: 10.1208/s12249-014-0202-z

Research Article

Multifunctional Nanoparticles for Prostate Cancer Therapy

Shantanu S. Chandratre[1] and Alekha K. Dash[1,2]

Received 4 June 2014; accepted 7 August 2014; published online 5 September 2014

Abstract. The relapse of cancer after first line therapy with anticancer agents is a common occurrence. This recurrence is believed to be due to the presence of a subpopulation of cells called cancer stem cells in the tumor. Therefore, a combination therapy which is susceptible to both types of cells is desirable. Delivery of this combinatorial approach in a nanoparticulate system will provide even a better therapeutic outcome in tumor targeting. The objective of this study was to develop and characterize nanoparticulate system containing two anticancer agents (cyclopamine and paclitaxel) having different susceptibilities toward cancer cells. Both drugs were entrapped in glyceryl monooleate (GMO)-chitosan solid lipid as well as poly(glycolic-lactic) acid (PLGA) nanoparticles. The cytotoxicity studies were performed on DU145, DU145 TXR, and Wi26 A4 cells. The particle size of drug-loaded GMO-chitosan nanoparticles was 278.4 ±16.4 nm with a positive zeta potential. However, the PLGA particles were 234.5±6.8 nm in size with a negative zeta potential. Thermal analyses of both nanoparticles revealed that the drugs were present in noncrystalline state in the matrix. A sustained *in vitro* release was observed for both the drugs in these nanoparticles. PLGA blank particles showed no cytotoxicity in all the cell lines tested, whereas GMO-chitosan blank particles showed substantial cytotoxicity. The types of polymer used for the preparation of nanoparticles played a major role and affected the *in vitro* release, cytotoxicity, and uptake of nanoparticles in the all the cell lines tested.

KEY WORDS: cancer stem cells; cyclopamine; glyceryl monooleate; nanoparticles; PLGA.

INTRODUCTION

The National Cancer Institute defines prostate cancer as the cancer that forms in the tissues of prostate glands. In men, it is the second most frequently diagnosed cancer (1). In 2013, there were 238,590 new cases of prostate cancer and an estimated 29,720 deaths reported among men as a result of prostate cancer in the USA (2). It has been suggested that tumors possess two types of cells, differentiated cancer cells and a small subpopulation of cells known as the cancer stem cells (CSCs). The CSCs are responsible for tumor initiation, growth, and recurrence and have the ability of self-renewal as well as self-differentiation (3). This ability of the CSCs is governed by various signaling pathways, and one of such pathways is the Sonic Hedgehog pathway (3).

For the successful treatment of cancer, it is essential to eliminate the cancer stem cells which are responsible for the recurrence of tumors. A high degree of chemoresistance is observed in case of tumors involving cancer stem cells. Studies have shown that CSCs possess drug efflux pumps which drive out the chemotherapeutic agents and can affect their transport into the tumor cells (4,5). Thus, for a successful therapy, it is essential to have at least one chemotherapeutic agent which can disrupt the signaling pathways responsible for the growth and differentiation of CSCs. Combination therapy in cancer treatment involves co-administration of more than one chemotherapeutic agent, aiming at enhancing the therapeutic activity and minimizing the systemic toxicity. This combination therapy works by combining drugs of different mechanisms of action in order to avoid broad spectrum drug resistance. Furthermore, combination therapy substantially reduces the number of doses to be administered, thereby improving the patient compliance (6). In some cases, combination therapy has shown the ability to overcome multidrug resistance (6,7).

In the present study, two anticancer agents, cyclopamine and paclitaxel, having different mechanisms of action, were investigated. Cyclopamine is a steroidal alkaloid obtained from ground roots and rhizomes of *Veratrum californicum* belonging to the family Melanthiaceae. This plant also known as California false hellebore (8). Cyclopamine is an inhibitor of the Sonic Hedgehog pathway responsible for the growth and proliferation of cancer stem cells. It has been used in the treatment of pancreatic cancer (9), glioblastoma multiforme (10), and prostate cancer (11). The use of cyclopamine in combination with paclitaxel for cancer stem cell therapy has also been reported (11). The mechanism, by which cyclopamine acts, is disrupting the *smoothened* (Smo), a seven-transmembrane receptor, activity. It antagonizes the Smo activity by binding to its heptahelical bundle (12). This causes the inhibition of the SHh pathway, resulting in the downregulation of genes responsible for CSCs growth,

[1] Department of Pharmacy Sciences, School of Pharmacy and Health Professions, Creighton University, 2500 California Plaza, Omaha, Nebraska 68178, USA.
[2] To whom correspondence should be addressed. (e-mail: adash@creighton.edu)

maturation, and proliferation. Paclitaxel (Taxol), on the other hand, is obtained from the extract of the inner bark of Pacific Yew tree, *Taxus brevifolia* (family: Taxaceae) (13). It increases tubulin polymerization and inhibits the mitotic spindle formation resulting in cell cycle arrest (14). Paclitaxel has been shown to work on a wide range of cancer types (15–17).

The present research reports the development and characterization of polymeric nanoparticulate drug delivery system containing two anticancer agents with different mechanisms of action for targeting both differentiated as well as cancer stem cells in prostate cancer therapy.

MATERIALS AND METHODS

Materials

Commercial grade cyclopamine was purchased from LC Laboratories (Woburn, MA), and paclitaxel was purchased from Tecoland Corporation, USA. Glyceryl monooleate and poloxamer 407 were obtained from Spectrum Chemicals (New Brunswick, NJ). Polyvinyl alcohol (molecular weight (MW), 30,000–70,000), low molecular weight chitosan (MW, 10,000–12,000), HPLC grade dichloromethane, MTT reagent (3-(4,5-dimethyl-2-thiazolyl)-2,5-diphenyl-2H-tetrazolium bromide), sodium dodecyl sulfate (SDS), and dimethylformamide (DMF) required for cytotoxicity studies were purchased from Sigma Aldrich (Milwaukee, WI). Triton X was purchased from Sigma Aldrich (St. Louis, MO). Poly(glycolic-lactic) acid (PLGA) (L/G, 50:50; intrinsic viscosity, 0.89 dL/g) was purchased from Absorbable Polymers International (Pelham, AL). Optima LC/MS grade acetonitrile, water, and trifluoroacetic acid were purchased from Fischer Scientific (Fair Lawn, NJ). DU145 (differentiated prostate cancer cells) and DU145 TXR (prostate cancer stem cells) were received as a generous gift from Dr. E. T. Keller (University of Michigan). Wi26 VA4 (normal lung cells) were obtained from American Type Culture Collection (Manassas, VA). RPMI-1640 medium, modified Eagle medium (MEM), Dulbecco's phosphate-buffer saline (DPBS), fetal bovine serum (FBS) albumin, nonessential amino acids, sodium pyruvate, penicillin-streptomycin, and glutamic acid were purchased from Invitrogen (Carlsbad, CA). For hemolysis studies, mouse blood was used and obtained from Innovative Research Inc. (Novi, MI). A 0.9% (*w*/*v*) solution of normal saline was purchased from Ricca Chemical Company (Arlington, TX). The mounting solution Fluoroshield™ containing 4′,6-diamidino-2-phenylindole (DAPI) was purchased from Sigma Life Sciences (St. Louis, MO).

Preparation of Nanoparticles

A 2.4% (*w*/*v*) solution of chitosan was prepared by dissolving 0.3 g chitosan in 12.5 mL of 100 mM citric acid solution. Glyceryl monooleate (GMO; 5 g) was melted at 40°C. Cyclopamine (0.073 g or 2.8% *w*/*w*) and paclitaxel (0.109 g or 4% *w*/*w*) were dissolved in the molten GMO. A 2% (*w*/*v*) solution of poloxamer 407 was prepared by dissolving 0.25 g poloxamer in 12.5 mL of deionized water. This surfactant solution was added to the molten GMO mixture. This mixture was sonicated at 18 W for 2 min (Misonix sonicator 3000, Farmingdale, NY) to form the primary emulsion. The 2.4% (*w*/*v*) chitosan solution was then added to this primary emulsion. The resultant mixture was sonicated further at 18 W for 2 min to form the final nanoemulsion. This nanoemulsion was subjected to freeze drying using Millrock Technology (Kingston, NY) lyophilizer. Initially, the sample was frozen at −55°C. It was further subjected to the primary drying cycle (heating from −25 to 25°C over a period of 22 h at vacuum of 50 MT). This was followed by the secondary drying cycle (20°C for 4 h) to give a dry powder of nanoparticles.

PLGA (0.22 g) along with cyclopamine (0.041 g or 3.1% *w*/*w*) and paclitaxel (0.061 g or 4.6% *w*/*w*) was dissolved in dichloromethane (DCM). A 1% (*w*/*v*) solution of PVA was prepared in water. This solution was mixed with the organic phase and sonicated at 30 W for 2 min to form a primary emulsion. This emulsion was further subjected to one cycle of high pressure homogenization using Microfluidics M110P (Newtown, MA) at a pressure of 15,000 psi. The nanoemulsion thus obtained was mechanically stirred overnight in order to evaporate out the organic phase before drying. The resultant nanoparticles, devoid of DCM, were washed with water three times and then freeze dried.

Nanoparticle Characterization

The particle size (PS) and the zeta potential (ZP) of the nanoparticles was determined using the Brookhaven Zetameter (ZetaPlus, Brookhaven Instruments Corporation, Holtsville, NY). Briefly, 2.5 mg of nanoparticles were suspended in 10 mL of deionized water and each reading was taken in triplicate. Aqueous suspensions GMO-chitosan and PLGA nanoparticles were prepared having a concentration of 5 mg/mL.

The drug entrapment efficiencies of the GMO-chitosan and PLGA nanoparticles were determined by ultra-performance liquid chromatography (UPLC). Briefly, 5 mg of GMO-chitosan nanoparticles were dispersed in 1 mL methanol and sonicated on the water bath for 60 min, followed by centrifugation at 13,000 rpm for 5 min (AccuSpin™ Micro R, Fisher Scientific) to extract out the drugs from the polymeric matrix. In case of PLGA nanoparticles, 3 mg nanoparticles were dissolved in 1 mL DCM. After complete dissolution, the solvent was evaporated using nitrogen purge. The residue was reconstituted using 1 mL methanol and sonicated on the water bath for 60 min followed by centrifugation at 13,000 rpm for 5 min. The supernatant was filtered using 0.2-μm syringe filter and analyzed for the drug content using the UPLC. The UPLC separation and quantification of cyclopamine and paclitaxel was achieved using an Aquity BEH Phenyl column (2.1×100 mm, 1.7 μm) (Waters Aquity system, Milford, MA). The mobile phase consisted of acetonitrile: 0.2% (*v*/*v*) trifluoroacetic acid in water in the ratio 40:60 (*v*/*v*) at a flow rate of 0.5 mL/min. The effluents were monitored at the detector wavelength of 220 nm (cyclopamine) and 235 nm (paclitaxel). The standard curves were linear in the concentration range of 3.1–100 μg/mL, and the peak height was used to determine the unknown concentration of drugs from standard curves.

The *in vitro* release profiles of the two types of nanoparticles were determined by measuring the cumulative amount of drug released over a period of 7 days. A side-by-side water-jacketed glass diffusion chamber (PermeGear Inc., Hellertown,

PA) maintained at 37°C and separated by 0.1-μm polycarbonate membrane (Molecular weight cut off, 2,000 D, Spectra/Por® Dialysis Membrane) was used for the experiment. About 80 mg of GMO-chitosan nanoparticles and 110 mg of PLGA nanoparticles were dispersed in 3 mL of release medium (phosphate buffer saline (pH 7.4)+0.5% *w/v* of Tween 80) in the donor compartment at time zero. The receiver compartment was filled with 3 mL of fresh release medium. The entire release medium from the receiver compartment was collected and replaced by fresh medium at regular time intervals and the drug content in the release medium was analyzed using a validated Ultrahigh Pressure Liquid Chromatography (UPLC) method. *In vitro* release profiles of cyclopamine and PTX are shown in Fig. 1a, b.

The physical state of the drugs in the freeze-dried nanoparticles was studied using differential scanning calorimetry (DSC). Pure drugs, blank and drug-loaded GMO-chitosan, as well as PLGA nanoparticles were analyzed using the Differential Scanning Calorimeter (Shimadzu, DSC 60, Kyoto, Japan) and are depicted in Fig. 2a, b. Samples (around 5 mg) were sealed in aluminum pans and were heated from 23 to 300°C at a rate of 10°C/min with a nitrogen purge of 20 mL/min.

The Cytotoxicity Studies of GMO-Chitosan and PLGA Nanoparticles

The cellular toxicity of cyclopamine and paclitaxel drug solutions, GMO-chitosan, and PLGA nanoparticles was studied on DU145, DU145 TXR, and Wi26 A4 cells using the MTT toxicity assay, and the results are depicted in Fig. 3a–c. The cells were split and plated in 96-well plates having the seeding densities of 2.88×10^7 for DU145, 8.75×10^6 for DU145 TXR, and 2.05×10^7 for Wi26 VA4 and were incubated in a humidified chamber at 37°C in an atmosphere of 5% CO_2. After 24 h of plating, seven different concentrations of treatment solutions consisting of cyclopamine-paclitaxel drug solutions, vehicle control, blank and drug-loaded GMO-chitosan, as well as PLGA nanoparticles were prepared. All the plates were incubated for 4 h. After the incubation period, the treatment along with the media was removed from each well and was replaced with fresh media. The plates were incubated over a period of 24, 48, and 72 h. After each incubation period, the cells were treated with 30 μL of MTT solution (5 mg/mL) prepared in PBS and incubated for additional 4 h. After this incubation, the MTT treatment was removed and the cells were washed and treated with a solution of 20% (*w/v*) SDS solution: dimethylformamide in the ratio of 1:1. All the plates were kept on the incubator shaker (MaxQ 4450, Thermo Scientific) for 45 min at 37°C and were then analyzed on the microplate reader (Multiskan MCC) at 540 nm.

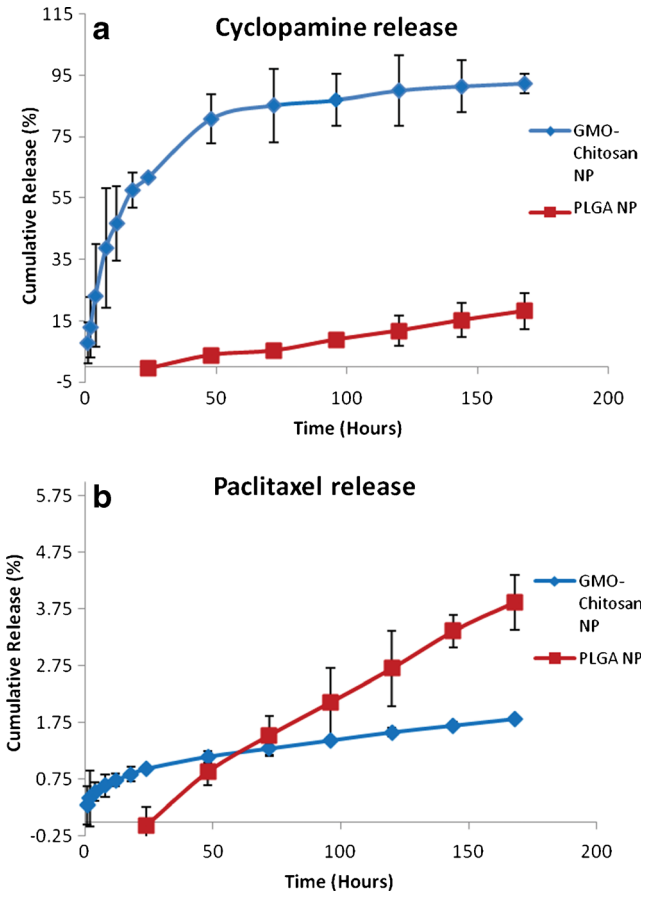

Fig. 1. *In vitro* release of cyclopamine (**a**) and paclitaxel (**b**) from GMO-chitosan and PLGA nanoparticles

Hemolytic Studies of GMO-Chitosan and PLGA Nanoparticles

Red blood cells (RBCs) were isolated from the whole blood of CD-1 mouse by centrifuging it at 1,000 rpm for 5 min (Sorvall® Legend RT). The supernatant serum fraction was discarded. The volume was made up to the initial volume of the whole blood using 0.9% (*w/v*) normal saline. The blood sample was centrifuged for 4–6 times until a clear supernatant was obtained. After the last cycle, the RBCs were diluted 1:10 with normal saline. This RBC solution (200 μL) was tested for hemolysis for drug solutions, vehicle, blank and drug-loaded GMO-chitosan, as well as PLGA nanoparticles. The volume of treatment used was 20/800 μL of normal saline. A 1% (*v/v*) solution of Triton X in normal saline was used as a positive control, whereas 0.9% (*w/v*) saline solution was used as a negative control. The treated RBCs were placed on the incubator shaker for 1 h. After the incubation period, the samples were centrifuged at 13,000 rpm for 5 min on the microcentrifuge. The supernatant was collected and was analyzed on the microplate reader at 404 and 540 nm. The percent hemolysis was calculated using the following formula:

$$\frac{\text{Sample absorbance-Blank Absorbance}}{\text{Absorbance of Positive Control}} \times 100$$

The percent hemolysis was calculated as a mean of two wavelengths (18,19).

The Cellular Association of GMO-Chitosan and PLGA Nanoparticles

The *in vitro* cellular association of the nanosystems was evaluated in DU145 and DU145 TXR human prostate cancer cells. The growth medium used for DU145 cells was RPMI-1640. The medium for DU145 TXR was RPMI-1640 supplemented with 10 nM paclitaxel. Both the media were supplemented with 20% (*v/v*) FBS, 10% (*v/v*) L-glutamine, 10% (*v/v*) nonessential amino acids,

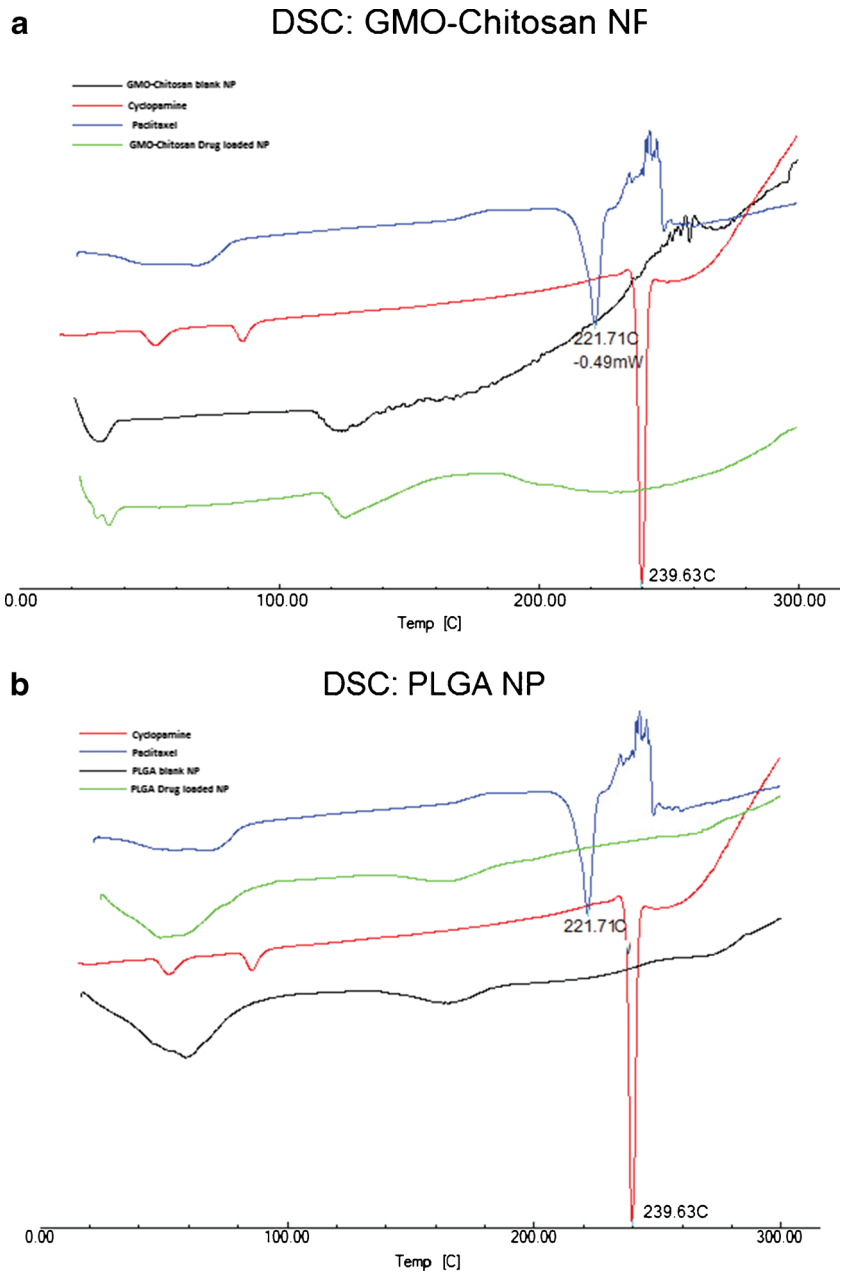

Fig. 2. An overlay plot of DSC thermograms for cyclopamine and paclitaxel (*pure drugs*) and blank and drug-loaded GMO-chitosan (**a**) and PLGA (**b**) nanoparticles

10% (*v*/*v*) penicillin streptomycin solution, and 10% sodium pyruvate. The cells were cultured in 6-well cell culture plates (Thermo Scientific Nunc^{TM}) at a seeding density of 2.88×10^7 for DU145 and 8.75×10^6 for DU145 TXR cells. The cells were plated and incubated at 37°C until they were confluent. A stock solution of cyclopamine and paclitaxel was prepared in RPMI-1640 medium using DMSO as the solvent. Suspensions of GMO-chitosan and PLGA nanoparticles containing equivalent content of drugs were prepared in RPMI-1640 medium. The confluent cells were treated with 2 mL of treatments prepared in the medium. After specified time intervals, the treatment was removed. The cells were washed three times with ice-cold phosphate buffer saline to remove the residual treatment. The cells were then lysed using mechanical scrapper. The lysates were collected in 2 mL microcentrifuge tubes and were homogenized using probe sonication. The homogenized lysates (20 μL) were analyzed for total protein content using the bicinchoninic acid (BCA) protein assay (Pierce, Rockford, IL). The remaining lysate was centrifuged at 13,000 rpm for 5 min. The supernatant was filtered through 0.2-μm syringe filter and analyzed using UPLC for cyclopamine and paclitaxel content. The cellular uptake was reported as mean±SD of cyclopamine and paclitaxel content per milligram of total cellular protein.

Subcellular Localization of PLGA Nanoparticles

The subcellular localization of PLGA nanoparticles tagged with a fluorescent marker (Rhodamine 6G) was studied in DU145 and DU145 TXR cells. In brief, DU145 and DU145 TXR cells were plated on BD Falcon 8-chamber slides at a seeding density of approximately 2.88×10^7 and 8.75×10^6, respectively. The cells were incubated for 36 h in a humidifying chamber at 37°C. After 24 h, the cells were treated with PLGA-Rhodamine nanoparticles suspended in RPMI-1640 media along with lysotracker green. The nanoparticle concentration was same as that used in the uptake studies. The cells were treated for 2.5 and 5 min. The treatment was removed, and the cells were washed three times with ice-cold DPBS and fixed with 1% (*v*/*v*) paraformaldehyde. After 10 min of incubation, the fixing agent was removed and the cells were washed once with ice-cold DPBS. The chamber partitions were removed, and the cells were stained with mounting solution Fluoroshield™ containing DAPI and sealed with cover slips. The slides were viewed under a Leica TCS SP8 multiphoton confocal microscope at the Integrated Biomedical Imaging Core Facility, Creighton University.

Statistical Analyses

The experimental data was statistically analyzed using a two tailed, unpaired equal variance Student's *t* test. The differences were termed statistically significant at $p<0.05$. Grubbs' test was used to determine and eliminate the outliers.

RESULTS

Preparation of Nanoparticles

GMO-chitosan blank as well as drug-loaded nanoemulsion prepared by double emulsion method was freeze-dried to obtain solid nanoparticles. PLGA nanoparticles (blank and drug-loaded) were prepared by emulsion and solvent evaporation method followed by freeze-drying.

Nanoparticle Characterization

The characterization of nanoparticles consisted of particle size, zeta potential, and entrapment efficiencies, and the results of these studies are depicted in Table I. The mean particle size ranged from 200 to 300 nm for both nanoparticle types. There was a significant difference ($p<0.05$) in the zeta potential of GMO-chitosan and PLGA nanoparticles (Table I). The entrapment of cyclopamine in GMO-chitosan nanoparticles was significantly higher ($p<0.05$) as compared to that in PLGA nanoparticles. However, no such difference was noticed in the case of paclitaxel (Table I).

The *in vitro* release of cyclopamine from the two polymeric systems is shown in Fig. 1a. It was observed that the release of cyclopamine from GMO-chitosan nanoparticles was significantly higher ($p<0.05$) than the release from PLGA nanoparticles. The release pattern was different in both of the formulations. There was an initial lag period seen in case of PLGA nanoparticles. Figure 1b represents the *in vitro* release characteristics of paclitaxel from the two polymeric systems. An initial lag phase was also observed in the case of paclitaxel release from PLGA nanoparticles. The release of cyclopamine was found to be significantly ($p<0.05$) higher than paclitaxel in GMO-chitosan nanoparticles.

Figure 2a represents the DSC thermograms of drugs along with blank and drug-loaded GMO-chitosan nanoparticles. The DSC curves of pure drugs showed two sharp endothermic melting peaks at around 240 and 222°C representing the melting peaks of cyclopamine and paclitaxel, respectively. These melting peaks were absent in both drug-loaded as well as the blank nanoparticles. Figure 2b represents the DSC thermograms of both drugs as well as blank and drug-loaded PLGA nanoparticles. No melting peaks for the drugs was observed in the drug-loaded as well as blank PLGA nanoparticles.

The Cytotoxicity Profile of GMO-Chitosan and PLGA Nanoparticles

Cytotoxicity profile of free cyclopamine-paclitaxel solution, blank and drug-loaded GMO-chitosan, and PLGA nanoparticles after 72 h of treatment in DU145, DU145 TXR, and Wi 26 A4 (C) cells are depicted in Fig. 3. The percentage survival of DU145 (Fig. 3a), DU145 TXR (Fig. 3b), and Wi26 VA4 (Fig. 3c) cells on treatment with cyclopamine-paclitaxel free drug solutions, blank and drug-loaded GMO-chitosan, as well as PLGA nanoparticles was studied overtime at various concentrations. Comparing the LD_{50} values in DU145 cells, it was observed that the blank GMO-chitosan was found to show greater cytotoxicity than the blank PLGA nanoparticles, whereas, on the other hand, the drug-loaded PLGA nanoparticles showed greater cytotoxicity than the drug-loaded GMO-chitosan nanoparticles as well as the drug solutions. In all of the three cell lines tested, the blank GMO-chitosan nanoparticles were found to be as cytotoxic as drug-loaded ones after 72 h of treatment. Hemolysis assay was further performed on various treatments, and the results are shown in Fig. 4. Blank and drug-loaded GMO-chitosan nanoparticles showed higher percentage of hemolysis as compared to the other treatments.

The Cellular Association of GMO-Chitosan and PLGA Nanoparticles

The cellular association of cyclopamine and paclitaxel in the formulation with comparison to solutions was determined in DU145 cells and shown in Fig. 5 and for DU145 TXR cells is shown in Fig. 6 by UPLC. The cellular uptake of cyclopamine in the solution form as well as in PLGA nanoparticles was found to be progressively increasing with time. PLGA nanoparticles showed peak uptake after 4 h of treatment in both the cell lines. The BCA protein analysis showed that the cells which were treated with GMO-chitosan nanoparticles showed low protein content after 2 h of treatment indicating cell lysis. Paclitaxel uptake showed no particular trend with time.

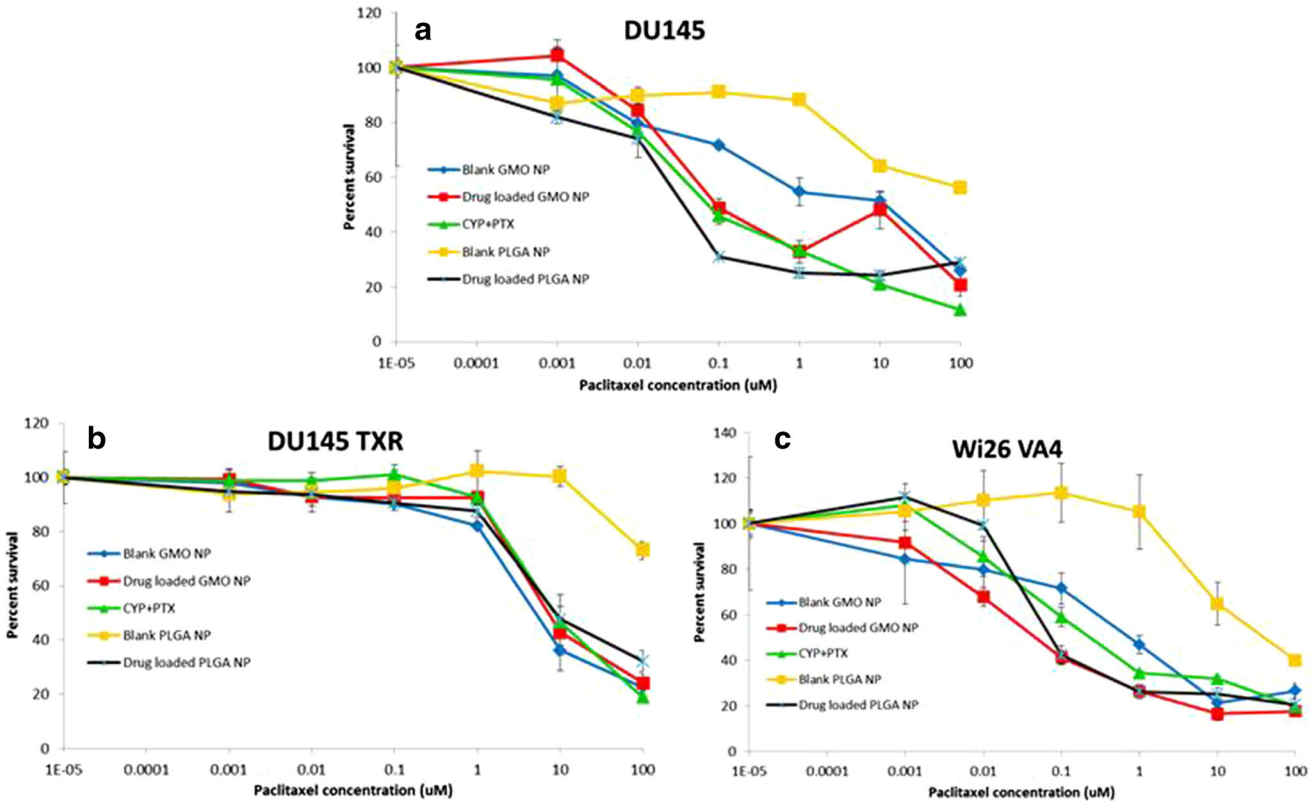

Fig. 3. Cytotoxicity profile of free cyclopamine-paclitaxel solution, blank and drug-loaded GMO-chitosan, and PLGA nanoparticles after 72 h of treatment in DU145 (**a**), DU145 TXR (**b**), and Wi 26 A4 (**c**) cells

Subcellular Localization of PLGA Nanoparticles

The subcellular localization of PLGA nanoparticles tagged with Rhodamine 6G was observed in DU145 and DU145 TXR cells using confocal microscopy and shown in Fig. 7. The cells were treated with the nanoparticles for 2.5 and 5 min. In both the cell lines, the nanoparticles appeared to start the process of internalization after 2.5 min. By the end of 5 min, the nanoparticles were completely taken up by the cells.

DISCUSSION

Our laboratory was previously involved in the development of GMO-chitosan nanoparticles for the delivery of hydrophilic as well as hydrophobic anticancer agents utilizing the bioadhesive properties of chitosan and GMO for targeting the cancer tissue (20,21). However, in the previous studies, we have only reported the targeting of drugs individually and not in combination. The present study further investigates the utility of not only GMO-chitosan but also PLGA nanosystem for the co-delivery of two hydrophobic anticancer agents having different mechanisms of action to target differentiated as well as cancer stem cells of prostate gland.

Nanoparticle Characterization

The size of both nanoparticle types was found to be in the range of 200 to 300 nm. There was no significant ($p<0.05$) difference observed in the particle size of drug-loaded GMO-chitosan and PLGA nanoparticles. In contrast to the previous studies with GMO-chitosan nanoparticles in our lab (20,21), the present study produced particles of smaller size. The

Table I. Physicochemical Characterization of Nanoparticles

Nanoparticles type	Particle size (nm)	Zeta potential (mV)	EE (% *w*/*w*)	
			CYP	PTX
GMO-chitosan blank	233.3±22.4	12.5±1.2	n/d	n/d
GMO-chitosan drug-loaded	278.4±16.4	10.1±1.4	83.6±3.9	88.8±4.3
PLGA-PVA blank	201.1±3.9	−8.0±0.7	n/d	n/d
PLGA-PVA drug-loaded	234.5±6.8	−0.9±0.5	55.3±0.5	86.4±0.9

Values are mean±SD; $n=3$
n/d not defined, *PTX* paclitaxel, *CYP* cyclopamine, *EE* entrapment efficiency

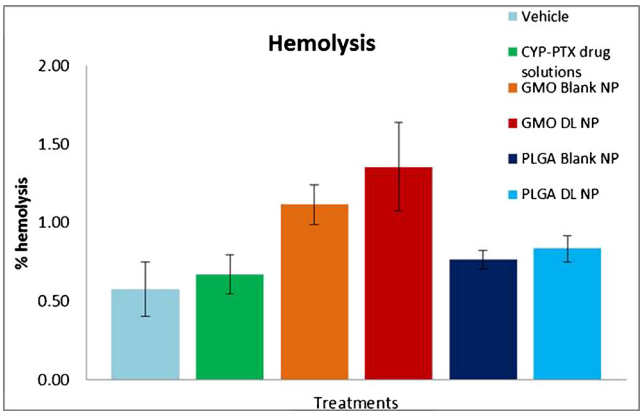

Fig. 4. Mean percent hemolysis of drug solutions, blank and drug-loaded GMO-chitosan, and PLGA nanoparticles

difference could possibly be attributed to the use of poloxamer as a stabilizer instead of PVA. A block copolymer such as poloxamer will exist in a different conformation around the GMO core than PVA leading to variations in particle size.

Chitosan is a naturally occurring cationic polysaccharide formed by the *N*-deacylation of chitin (22). This imparts a slight positive charge to the GMO-chitosan nanoparticles. PLGA polymer is known to have a high negative surface charge. However, the presence of PVA as a stabilizer lowers the negative charge as it shields the surface charge of PLGA and brings it close to zero (23).

In the GMO-chitosan nanoparticles, the entrapment of cyclopamine was found to be significantly ($p<0.05$) higher than in PLGA nanoparticles. One possible reason for this could be the fact that during the preparation of PLGA nanoparticles, a washing step was involved, unlike in the preparation of GMO-chitosan nanoparticles.

The physical state of drugs in the nanoparticles affects the *in vitro* release patterns. If the drugs are present in an amorphous or noncrystalline form, they can diffuse through the polymer matrix and show a sustained release as compared to their crystalline counterpart (24). The DSC analysis showed endothermic melting peaks of both cyclopamine and paclitaxel at 221.71 and 239.63°C, respectively (Fig. 2). These values corresponded to the melting point values for these drugs published in the literature (http://pubchem.ncbi.nlm.nih.gov/) (25). Melting peaks were not observed for either of the drugs in GMO-chitosan or in PLGA nanoparticles, suggesting that the drugs encapsulated in the nanoparticles are in amorphous, disordered crystalline, or in solid-state solubilized form in the polymer matrix. An endothermic peak observed at around 37°C in the DSC thermograms of blank and drug-loaded GMO-chitosan nanoparticles may represent the melting of glyceryl monooleate (26).

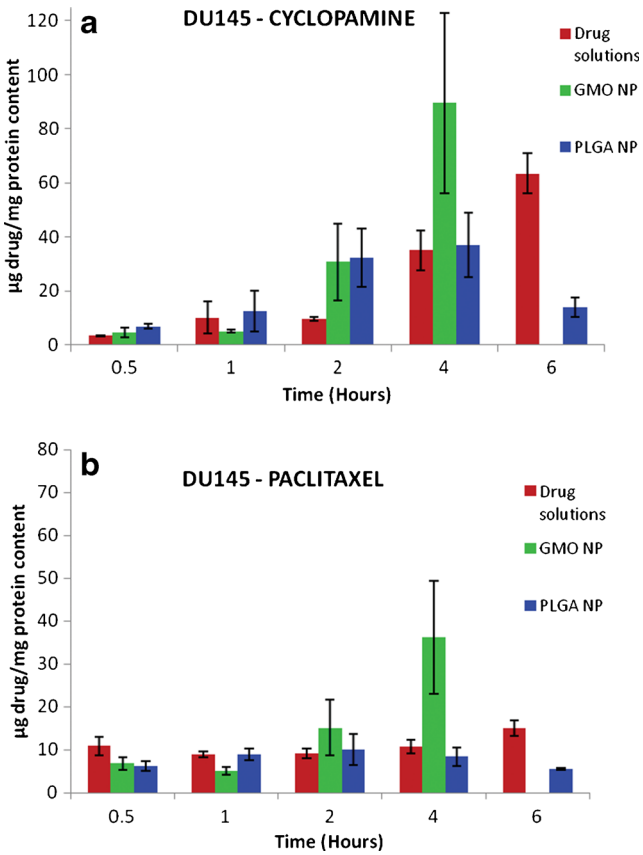

Fig. 5. Cellular uptake of cyclopamine (**a**) and paclitaxel (**b**) from drug solutions as well as nanoparticle formulations in DU145 cells

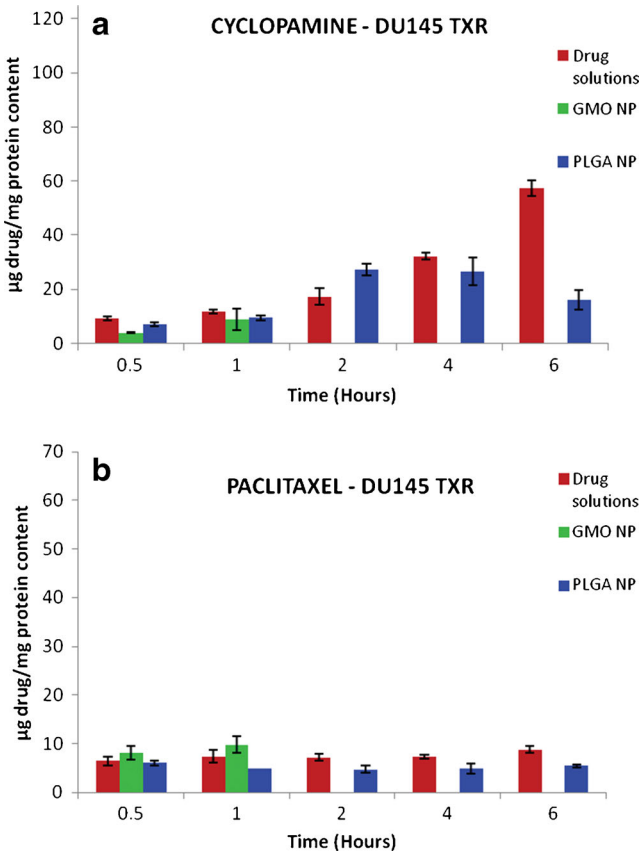

Fig. 6. Cellular uptake of cyclopamine (**a**) and paclitaxel (**b**) from drug solutions as well as nanoparticle formulations in DU145 TXR cells

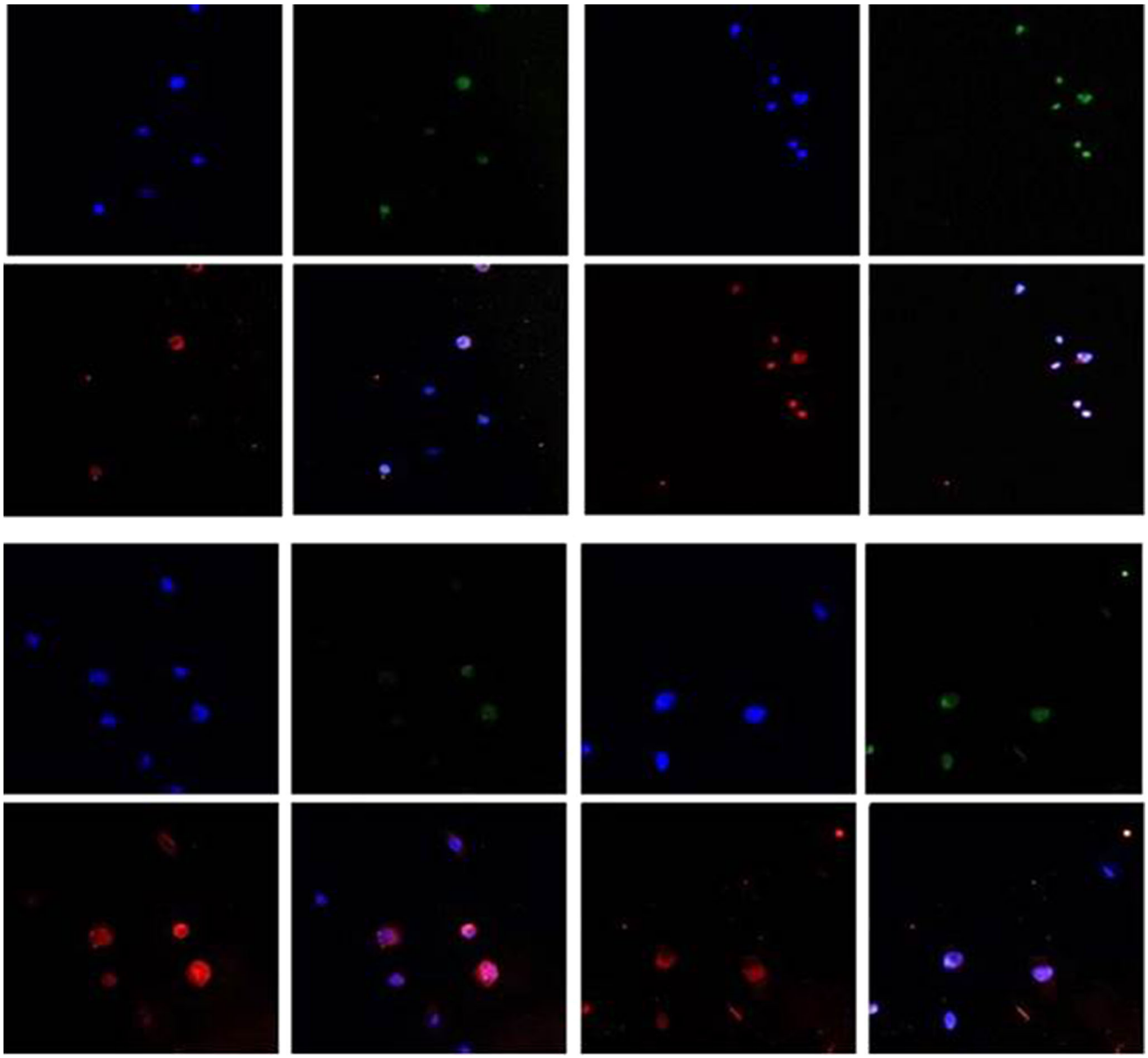

Fig. 7. Localization of PLGA nanoparticles in DU145 cells after 2.5 min (**a**) and 5 min (**b**) and in DU145 TXR cells after 2.5 min (**c**) and 5 min (**d**) of treatment

In Vitro Release

Several factors such as physicochemical properties of entrapped drugs, nature of the core, strength of the interactions between the drugs, and the core materials play an important role in governing the drug release pattern from a delivery system (27). The release of cyclopamine was found to be higher than paclitaxel in both types of nanoparticles in spite of cyclopamine having higher log *p* value. Similar results were reported by Cho *et al.* (28). The relative rapid release of cyclopamine as compared to paclitaxel could possibly be because of the higher affinity of paclitaxel toward both the polymeric systems over cyclopamine. This might have led to slower release of paclitaxel as compared to cyclopamine. Another possible reason for these results could be the greater equilibrium solubility of cyclopamine in the release media than paclitaxel. In GMO-chitosan nanoparticles, cyclopamine showed a burst release within the first 24 h of the experiment. This was followed by a sustained release for the next 6 days. Cyclopamine showed lower entrapment than paclitaxel in GMO-chitosan nanoparticles. The drug which is not entrapped within the nanoparticles might possibly be adsorbed on the chitosan layer. Since chitosan is hydrophilic in nature, it might be preventing the hydrophobic cyclopamine from excessive surface-binding leading to rapid initial burst release. Another possible explanation for rapid burst release could be the tendency of chitosan to swell in aqueous media, leading to increased water penetration in the system (20). In PLGA nanoparticles, cyclopamine had an initial lag phase for the first 24 h which was followed by a sustained release. Paclitaxel had a higher release from PLGA

nanoparticles than in GMO-chitosan nanoparticles. One possible reason for this slow release from GMO-chitosan nanoparticles could be the high affinity of paclitaxel for the lipophilic core consisting of GMO. This may retard the overall release of paclitaxel in the aqueous media.

The Cytotoxicity Profile and Hemolysis Assay of GMO-Chitosan and PLGA Nanoparticles

MTT assay was performed on prostate cancer (DU145 and DU145 TXR) and normal human (Wi26 VA4) cells to assess the *in vitro* cytotoxicity of cyclopamine-paclitaxel drug solutions in comparison to blank as well as drug-loaded GMO-chitosan and PLGA nanoparticles (Fig. 3). Blank GMO-chitosan nanoparticles were found to be as cytotoxic as the drug-loaded ones in all the three cell lines tested. However, our previously reported MTT assays with chitosan/GMO blank nanoparticles with human breast cancer cells (MDA-MB-321) (20) as well as pancreatic cancer cells (MIA PaCa-2 and BxPC-3) (21) have shown minimal cytotoxicity. This difference in cellular response with blank chitosan/GMO nanoparticles could be due to cell specificity. No such cytotoxic effects were observed with blank PLGA nanoparticles on either of the cell lines. After 24 h of treatment, drug-loaded PLGA nanoparticles showed less toxicity than drug solutions and GMO-chitosan nanoparticles in normal human cells (Wi26 A4), proving its specificity toward cancer cells. Hemolysis assay was performed on drug solutions, GMO-chitosan, and PLGA nanoparticles. No hemolysis was observed in blood samples treated with nanoparticle suspensions of both kinds. This study ensured that the formulations were safe for intravenous administration.

The Cellular Association and Subcellular Localization

Nanoparticles are known to show an increase in the intracellular drug concentration via energy-dependent processes of internalization like endocytosis (21,29,30). GMO-chitosan nanoparticles have shown to possess bioadhesion properties (20). This property may play a role in the enhanced cellular association. Coating antisense oligonucleotide to the PLGA particles have been reported to show an enhanced uptake (31). The PLGA nanoparticles tend to rapidly escape into the cell cytoplasm immediately after internalization. Once the particles enter the cytoplasm, they deliver the entrapped drug in a sustained manner (29). In the present study, the cellular uptake of GMO-chitosan and PLGA nanoparticles *versus* drug solutions was studied in DU145 and DU145 TXR prostate cancer cells. When observed under the optical microscope, the cells which were treated with GMO-chitosan nanoparticles started to show lysis in the form of disruption of cell membrane after 2 h of treatment. These observations were supported by low protein content values obtained after BCA protein analysis. Cyclopamine showed higher release than paclitaxel in both the formulations over a period of 7 days. This could explain the progressive increase and higher uptake of cyclopamine over time in comparison to paclitaxel in both the cell lines tested.

CONCLUSION

In conclusion, the current study dealt with the development and characterization of GMO-chitosan solid lipid nanoparticle system containing cyclopamine and paclitaxel for targeting differentiated as well as cancer stem cells in prostate gland. Both the drugs showed high entrapment in the nanoparticles. The nanoparticles showed a uniform size distribution. The drugs were released in a sustained manner over a period of 7 days. An alternate polymeric system consisting of PLGA was also developed and characterized. This carrier system proved to be much more efficient for targeting the prostate cancer cells. It showed a better cytotoxicity profile than the GMO-chitosan nanoparticles. Thus, it can be concluded that the type of carrier systems used for the preparation of nanoparticles play a major role in the *in vitro* release, cytotoxicity, and uptake of nanoparticles in the prostate cancer cells.

ACKNOWLEDGMENTS

We would like to acknowledge Dr. E. T. Keller (University of Michigan) for generously providing us with DU145 (differentiated prostate cancer cells) and DU145 TXR (prostate cancer stem cells) and Dr. Richard Hallworth, Integrated Biomedical Imaging Core Facility, Creighton University for the help in confocal microscopy.

REFERENCES

1. Jemal A, Bray F, Ferlay J. Glob Cancer Stat. 2011;61(2):69–90.
2. American Cancer Society Facts & Figs. 2013, Atlanta GA. 2013
3. Wang K, Wu X, Wang J, Huang J. Cancer stem cell theory: therapeutic implications for nanomedicine. Int J Nanomedicine [Internet]. 2013;8:899–908. Available from: http://www.pubmedcentral.nih.gov/articlerender.fcgi?artid=3589204&tool=pmcentrez&rendertype=abstract.
4. Gottesman MM, Fojo T, Bates SE. Multidrug resistance in cancer: role of ATP-dependent transporters. Nat Rev Cancer [Internet]. 2002;2(1):48–58. Available from: http://www.ncbi.nlm.nih.gov/pubmed/11902585.
5. Kim M, Turnquist H, Jackson J, Sgagias M, Yan Y, Gong M, *et al.* The multidrug resistance transporter ABCG2 (breast cancer resistance protein 1) effluxes Hoechst 33342 and is overexpressed in hematopoietic stem cells. Advances in Brief The multidrug resistance transporter ABCG2 (breast cancer resistance protein 1) E. 2002;2:22–8
6. Pinto AC, Moreira JN, Simões S. Combination chemotherapy in cancer: principles, evaluation and drug delivery strategies. 2010
7. Chou T-C. Drug combination studies and their synergy quantification using the chou-talalay method. Cancer Res [Internet]. 2010;70(2):440–6. Available from: http://www.ncbi.nlm.nih.gov/pubmed/20068163.
8. Heretsch P, Tzagkaroulaki L, Giannis A. Cyclopamine and hedgehog signaling: chemistry, biology, medical perspectives. Angew Chem Int Ed Engl [Internet]. 2010;49(20):3418–27. Available from: http://www.ncbi.nlm.nih.gov/pubmed/20429080.
9. Chitkara D, Singh S, Kumar V, Danquah M, Behrman SW, Kumar N, *et al.* Micellar delivery of cyclopamine and gefitinib for treating pancreatic cancer. Mol Pharm [Internet]. 2012; Available from: http://www.ncbi.nlm.nih.gov/pubmed/22780906
10. Vescovi AL, Dimeco F, Olivi A, Charles G. Cyclopamine-mediated hedgehog pathway inhibition depletes stem-like cancer cells in glioblastoma. Ste Cells. 2008;25(10):2524–33.
11. Singh S, Chitkara D, Mehrazin R, Behrman SW, Wake RW, Mahato RI. Chemoresistance in prostate cancer cells is regulated

by miRNAs and hedgehog pathway. PLoS One [Internet]. 2012;7(6):e40021. Available from: http://www.pubmedcentral.nih.gov/articlerender.fcgi?artid=3386918&tool=pmcentrez&rendertype=abstract.
12. Kumar SK, Indrajit R, Anchooria RK, Fazlia S, Anirban M, Beachyc PA, *et al*. Targeted inhibition of hedgehog signaling by cyclopamine prodrugs for advanced prostate cancer. Bioorg Med Chem. 2009;16(6):2764–8.
13. Zabaleta V, Ponchel G, Salman H, Agüeros M, Vauthier C, Irache JM. Oral administration of paclitaxel with pegylated poly(anhydride) nanoparticles: permeability and pharmacokinetic study. Eur J Pharm Biopharm [Internet]. 2012;81(3):514–23. Available from: http://www.ncbi.nlm.nih.gov/pubmed/22516136.
14. Cai J, Zheng T, Masood R, Smith DL, Hinton DR, Kim CN, *et al*. Paclitaxel induces apoptosis in AIDS-related Kaposi's sarcoma cells. Sarcoma [Internet]. 2000;4(1–2):37–45. Available from: http://www.pubmedcentral.nih.gov/articlerender.fcgi?artid=2408359&tool=pmcentrez&rendertype=abstract.
15. Nie S, Hsiao WLW, Pan W, Yang Z. Thermoreversible Pluronic F127-based hydrogel containing liposomes for the controlled delivery of paclitaxel: in vitro drug release, cell cytotoxicity, and uptake studies. Int J Nanomedicine [Internet]. 2011;6:151–66. Available from: http://www.pubmedcentral.nih.gov/articlerender.fcgi?artid=3075891&tool=pmcentrez&rendertype=abstract.
16. Schiff PB, Fant J, Horwitz S. Promotion of microtubule assembly in vitro by taxol. Nat. 1979;277(5698):665–7.
17. Tishler RB, Geard CR, Hall EJ, Schiff P. Taxol sensitizes human astrocytoma cells to radiation. Cancer Res. 1992;52(12):3495–7.
18. Plumel M. Bull Soc Chim Biol. 1949;30:129.
19. Go M, Liu M, Wilairat P, Rosenthal PJ, Saliba KJ, Kirk K. Antiplasmodial chalcones inhibit sorbitol-induced hemolysis of plasmodium falciparum-infected erythrocytes. Antimicrob Agents Chemother. 2004;48(9):3241–5.
20. Trickler WJ, Nagvekar AA, Dash AK. A novel nanoparticle formulation for sustained paclitaxel delivery. AAPS PharmSciTech [Internet]. 2008;9(2):486–93. Available from: http://www.pubmedcentral.nih.gov/articlerender.fcgi?artid=2976931&tool=pmcentrez&rendertype=abstract.
21. Trickler WJ, Khurana J, Nagvekar A, Dash AK. Chitosan and glyceryl monooleate nanostructures containing gemcitabine: potential delivery system for pancreatic cancer treatment. AAPS PharmSciTech [Internet]. 2010;11(1):392–401. Available from: http://www.pubmedcentral.nih.gov/articlerender.fcgi?artid=2850475&tool=pmcentrez&rendertype=abstract.
22. Carneiro-da-Cunha MG, Cerqueira M, Souza BWS, Teixeira J, Vicente A. Influence of concentration, ionic strength and pH on zeta potential and mean hydrodynamic diameter of edible polysaccharide solutions envisaged for multinanolayered films production. Carbohydr Polym [Internet]. 2011;85(3):522–8. Available from: http://linkinghub.elsevier.com/retrieve/pii/S0144861711001640.
23. Sahoo SK, Panyam J, Prabha S, Labhasetwar V. Residual polyvinyl alcohol associated with poly (D, L-lactide-co-glycolide) nanoparticles affects their physical properties and cellular uptake. J Control Release [Internet]. 2002;82(1):105–14. Available from: http://www.ncbi.nlm.nih.gov/pubmed/12106981.
24. Mohanty C, Sahoo SK. The in vitro stability and in vivo pharmacokinetics of curcumin prepared as an aqueous nanoparticulate formulation. Biomater [Internet]. 2010;31(25):6597–611. Available from: http://www.ncbi.nlm.nih.gov/pubmed/20553984.
25. Liggins RT, Hunter WL, Burt HM. Solid-state characterization of paclitaxel. J Pharm Sci [Internet]. 1997;86(12):1458–63. Available from: http://www.ncbi.nlm.nih.gov/pubmed/18167583.
26. Ganem-Quintanar A, Quintanar-Guerrero D, Buri P. Monoolein: a review of the pharmaceutical applications. Drug Dev Ind Pharm [Internet]. 2000;26(8):809–20. Available from: http://www.ncbi.nlm.nih.gov/pubmed/10900537.
27. Chitkara D, Singh S, Kumar V, Danquah M, Behrman SW, Kumar N, *et al*. Micellar delivery of cyclopamine and gefitinib for treating pancreatic cancer. Mol Pharm [Internet]. 2012;9(8):2350–7. Available from: http://www.ncbi.nlm.nih.gov/pubmed/22780906.
28. Cho H, Lai TC, Kwon GS. Poly(ethylene glycol)-block-poly(ε-caprolactone) micelles for combination drug delivery: evaluation of paclitaxel, cyclopamine and gossypol in intraperitoneal xenograft models of ovarian cancer. J Control Release [Internet]. 2013;166(1):1–9. Available from: http://www.ncbi.nlm.nih.gov/pubmed/23246471.
29. Panyam J, Zhou W-Z, Prabha S, Sahoo SK, Labhasetwar V. Rapid endo-lysosomal escape of poly (DL-lactide-co-glycolide) nanoparticles: implications for drug and gene delivery. FASEB J [Internet]. 2002;16(10):1217–26. Available from: http://www.ncbi.nlm.nih.gov/pubmed/12153989.
30. Rejman J, Oberle V, Zuhorn IS, Hoekstra D. Size-dependent internalization of particles via the pathways of clathrin- and caveolae-mediated endocytosis. Biochem J [Internet]. 2004;377(Pt 1):159–69. Available from: http://www.pubmedcentral.nih.gov/articlerender.fcgi?artid=1223843&tool=pmcentrez&rendertype=abstract.
31. Nafee N, Taetz S, Schneider M, Schaefer UF, Lehr C-M. Chitosan-coated PLGA nanoparticles for DNA/RNA delivery: effect of the formulation parameters on complexation and transfection of antisense oligonucleotides. Nanomedicine [Internet]. 2007;3(3):173–83. Available from: http://www.ncbi.nlm.nih.gov/pubmed/17692575.